

Key Points:

- Seawater humic-like substances (HULIS) concentrations consistently increase during phytoplankton blooms, but remain mostly in the $<0.2 \mu\text{m}$ or $<50 \text{ kDa}$ size fraction
- High bacterial enzymatic activity in seawater enhances HULIS production
- HULIS chemical changes may play a role in HULIS sea-air transfer

Supporting Information:

Supporting Information may be found in the online version of this article.

Correspondence to:

K. A. Prather,
kprather@ucsd.edu

Citation:

Santander, M. V., Malfatti, F., Pendergraft, M. A., Morris, C., Kimble, K., Mitts, B. A., et al. (2023). Bacterial control of marine humic-like substance production, composition, size, and transfer to sea spray aerosols during phytoplankton blooms. *Journal of Geophysical Research: Atmospheres*, 128, e2022JD036869. <https://doi.org/10.1029/2022JD036869>

Received 1 APR 2022

Accepted 29 JAN 2023

Bacterial Control of Marine Humic-Like Substance Production, Composition, Size, and Transfer to Sea Spray Aerosols During Phytoplankton Blooms

Mitchell V. Santander¹, Francesca Malfatti^{2,3,4}, Matthew A. Pendergraft⁴, Clare Morris^{1,4}, Ke'La Kimble¹, Brock A. Mitts¹ , Xiaofei Wang⁵ , Kathryn J. Mayer¹, Jon Sauer¹ , Christopher Lee⁴ , and Kimberly A. Prather^{1,4} 

¹Department of Chemistry and Biochemistry, University of California, San Diego, La Jolla, CA, USA, ²University of Trieste, Trieste, Italy, ³Istituto Nazionale di Oceanografia e di Geofisica Sperimentale (OGS), Borgo Grotta Gigante, Italy, ⁴Scripps Institution of Oceanography, University of California, San Diego, La Jolla, CA, USA, ⁵Department of Environmental Science and Engineering, Fudan University, Shanghai, China

Abstract Humic-like substances (HULIS) are present in every environmental reservoir, including the ocean and the atmosphere. Ocean-derived HULIS can be transferred to the atmosphere in the form of sea spray aerosols (SSA). Little information exists on the factors controlling this transfer process or how HULIS alter SSA physicochemical properties, cloud-forming ability, and atmospheric reactions. Here, using excitation-emission matrix spectroscopy and isolated ocean-atmosphere systems, we investigated how ocean biology affects HULIS sea-to-air transfer during multiple phytoplankton bloom experiments. We posit that bacterial enzymatic activity on phytoplankton-derived organic matter control HULIS size, production, and chemical composition. We found that changes in fluorescence indices and shifts in the HULIS fluorescence emission spectra reveal changes in HULIS chemical composition induced by bacteria. High bacterial enzymatic activity on the proteinaceous, lipid, and phosphorus-rich organic pools enhanced HULIS production and its transfer to SSA. Seawater HULIS consistently accumulated across all experiments. The majority of HULIS was smaller than $0.2 \mu\text{m}$ or 50 kDa . Our results suggest that enzymatic-processing bacteria transform the composition of HULIS in seawater, degrading dissolved organic matter into diverse chemical structures that are more efficiently transferred to the atmosphere in SSA.

Plain Language Summary Humic-like substances (HULIS) are complex molecules found in the ocean. When waves break, HULIS can be launched into the atmosphere in tiny sea spray aerosol particles (SSA). While it is well documented that bacteria modify molecules in the ocean, far less is known about how they modify the characteristics and ocean-to-atmosphere transfer of HULIS. Here, we use a laboratory ocean-atmosphere simulator to study how ocean biology affects HULIS properties in air and ocean samples. We found associations between ocean enzyme activities, HULIS chemistry, and the relative abundance of HULIS in SSA. Therefore, this study shows that marine bacteria enzymes can modify the chemical structures of HULIS, which in turn impacts their ability to transfer to the air via SSA. This study provides insight into the complex role marine biology plays in affecting SSA composition which controls marine clouds and climate.

1. Introduction

Humic-like substances (HULIS) are ubiquitous in all natural environments including the soil, oceans, and the atmosphere (Graber & Rudich, 2006; Hessen & Tranvik, 1998; Rashid, 1985). They consist of a complex mixture of organic molecules that are generated during the breakdown of dead organisms and larger biomolecules (Hessen & Tranvik, 1998; Rashid, 1985). HULIS in aerosol particles (Graber & Rudich, 2006) influence cloud formation and lifetime and atmospheric composition (Borgatta & Navea, 2015; Chen et al., 2021; Slade et al., 2017; Stemmler et al., 2007). It has been postulated that the ocean is the main source of atmospheric HULIS in sea spray aerosols (SSA) generated by breaking waves (Cavalli et al., 2004; Gruber & Rudich, 2006). Many studies investigating the sea-air transfer of organic matter have recognized that marine microbes, specifically interactions between phytoplankton production and bacterial enzymatic activities, play a critical role in controlling SSA chemistry (Freney et al., 2021; Lee et al., 2015; Malfatti et al., 2019; O'Dowd et al., 2015; Prather et al., 2013; Wang et al., 2015). Previous laboratory experiments have shown that HULIS concentrations in bulk seawater are different from concentrations in SSA, suggesting other factors besides seawater abundance control

Table 1

List of the Experiments Probing the Dynamics of Humic-Like Substances

Name	Year	Tank system	SSA generator	System volume (L)	SSA collection	Duration (days)	Peak CHL (µg/L)	Bulk seawater measurements					Enzyme activity
								CHL	HB	V	DOC		
Exp1	2014	Wave-flume	Wave-flume	30,000	Imp	37	5.76	X	X	X	X	X	
Exp2	2019	Wave-flume	Wave-flume	30,000	Spot	21	18.70	X	X	X	X	X	
Exp3	2018	Outdoor Tank/MART	MART	100	Spot	9	12.65	X	X	X	X	X	
Exp4	2018	Outdoor Tank/MART	MART	100	Spot	9	11.41	X	X	X	X	X	
Exp5	2014	MART	MART	100	Imp	26	39.08	X	--	--	X	--	
Exp6	2014	MART	MART	100	Imp	19	13.10	X	--	--	X	--	
Exp7	2019	Outdoor Tank/MART	MART	100	Spot	9	1.90	X	X	X	--	--	

Note. Experiments designated as Exp1–7 are experiments where EEMs were collected for both bulk seawater and SSA. HB = heterotrophic bacterial abundances, V = viral abundances, DOC = dissolved organic carbon, and CHL = in vivo or extracted chlorophyll; Imp = impingers, Spot = Spot sampler.

atmospheric HULIS concentrations (Santander et al., 2022). However, controlled studies of the chemical and biological factors that control the production, chemical composition, and size of HULIS and their transfer to SSA have yet to be probed.

In this study, we used excitation emission matrix (EEM) spectroscopy to characterize marine-derived HULIS and investigate the mechanisms that regulate the transfer of HULIS from seawater to SSA (Mostofa, 2013; Murphy et al., 2013; Nebbiosi & Piccolo, 2013). EEM spectroscopy acquires fluorescence emission spectra at multiple excitation wavelengths, which are concatenated to form a single excitation–emission matrix. EEMs allow for rapid, direct measurements of the fluorescent organic matter in seawater without requiring sample storage or preprocessing. By concatenating multiple excitation wavelengths, EEMs can characterize multiple classes of fluorophores within each sample, including protein-like substances and chlorophyll in seawater (Coble, 2007; Mostofa, 2013; Parlanti et al., 2000). This study focuses solely on HULIS fluorescence in seawater and SSA. Previous studies have identified HULIS by a broad fluorescence peak with an excitation wavelength of 360 nm and emission wavelengths ranging from 430 to 470 nm (Lee et al., 2015; Pohlker et al., 2012). By monitoring this peak over time, changes in HULIS concentrations and chemical composition can be investigated in seawater and SSA.

Here we hypothesize that bacterial enzymes alter the production, chemical composition, and size of HULIS, and that these changes modify the efficiency of HULIS transfer from the ocean to the atmosphere in SSA. We performed experiments to disentangle the impact of phytoplankton, bacteria, and bacterial enzymes on HULIS composition and transfer. Controlled phytoplankton bloom experiments allowed for the investigation of HULIS properties under phytoplankton and bacterial growth cycles of varying bloom intensities. Perturbation experiments, where marine bacterial isolates were added, help clarify the role of bacteria and their enzymes on HULIS composition. Specifically, we examined the impact of proteases (cleavage site leucine), lipases (cleavage site oleate), and alkaline phosphatases (cleavage site phosphate), which have been shown to be relevant for sea-air transfer of organic matter (Malfatti et al., 2019). We then probed the impact of these enzymes on seawater HULIS properties, and how this affects HULIS transfer from seawater to SSA. While studies have shown that phytoplankton blooms affect seawater and SSA chemistry (Lee et al., 2015; Prather et al., 2013; Wang et al., 2015), this study goes beyond phytoplankton and provides new insights into the links between bacterial enzyme activity and HULIS production, physicochemical properties and sea-air transfer.

2. Methods

2.1. Phytoplankton Bloom Experiments

Seventeen phytoplankton bloom experiments were conducted using natural seawater (Table 1, Tables S1 and S2 in Supporting Information S1). Seawater collected from the Ellen Browning Scripps Memorial Pier (32°52'00"N, 117°15'21"W) was filtered using an acid washed 50 µm mesh screen (Sefar Nitex 03–100/32) to remove

zooplankton grazers of phytoplankton in order to promote algae growth and better control the microbial dynamics. In the experiments discussed here, three mesocosm conditions were employed; seawater was (a) placed directly into a 120 L Marine Aerosol Reference Tank (MART) (Stokes et al., 2013), (b) placed into a 3000 L outdoor tank to allow phytoplankton abundance to increase, followed by aerosolization in a MART (Trueblood et al., 2019), or (c), placed in a 30,000 L waveflume at Scripps Institution of Oceanography (Table 1, Table S1 in Supporting Information S1). In the seven experiments labeled as Exp1–7, HULIS was sampled in the bulk seawater (total and size fractionated) and in the SSA (Table 1). Exp1, or the Investigation into Marine PArticle Chemistry and Transfer Science (IMPACTS) campaign (Wang et al., 2015), and Exp2, or the Sea Spray Chemistry and Particle Evolution (SeaSCAPE) campaign (Sauer et al., 2022), were conducted in the waveflume, while Exp3–7 used the MART for SSA generation. In the 10 experiments labeled as S01–S10, total HULIS were sampled only in the bulk seawater (Table S1 in Supporting Information S1). Methods used for phytoplankton mesocosm experiments in both the waveflume and the MARTs have been described previously (Lee et al., 2015; Wang et al., 2015). Briefly, the seawater was spiked with Guillard's F/2 algae nutrient medium (Guillard & Ryther, 1962) (concentrations ranging from F/100 to F/2) to induce a phytoplankton bloom and then incubated with fluorescent lights (Full Spectrum Solutions, model 205457; T8 format, color temperature 5700 K, 2,950 lumens) (Brown & Richards, 1968). Experiments carried out in the outdoor tank used sunlight rather than fluorescent lights for incubation. The growth and decline of phytoplankton were monitored daily using an Aquafluor handheld fluorometer (Turner Designs, Aquafluor) to measure *in vivo* chlorophyll-a fluorescence (excitation at 395 nm and emission \geq 660 nm).

For Exp4, marine bacteria isolates were introduced into the MART after the peak of the phytoplankton bloom. Three different marine bacteria isolates were used: *Alteromonas macleodii* (AltSIO), *Pseudoalteromonas* sp. (ATW7), and *Flavobacteria* sp. (BBFL7). These three strains were chosen due to their high protease activities that, in previous studies, were found to be effective in the dissolution of particulate silica present in diatom frustule (Bidle & Azam, 2001). AltSIO was also added due to its ability to breakdown dissolved organic carbon (DOC), as shown previously (Pedler et al., 2014). These three “local” species were originally isolated from the Pacific Ocean off of the Ellen Browning Scripps Memorial Pier. The bacterial isolates were prepared by growing colonies on solid ZoBell medium at room temperature from the frozen stock culture for 24 hr (Sambrook et al., 1989). Colonies were then transferred to liquid ZoBell medium at room temperature and grown on a shaker at 130 rpm for approximately 24 hr. Liquid cultures were harvested by spinning at 9,000 g for 5 min, followed by a wash with 0.2 μ m filtered and sterilized seawater to remove the supernatant (spent medium). Optical density measured at 600 nm was checked in order to have 1:1:1 (AltSIO:ATW7:BBFL7) ratio of the isolates in the inoculum that was 1×10^9 cells/L (Azam et al., 1983). The final concentration of bacteria in the MART was targeted to be double that of the existing concentration, while still on the order of 10^9 cells per liter. We chose to double the bacteria abundance in order to perturb the system thus creating a step change in seawater chemistry (e.g., enhancing degradative enzymatic activities).

2.2. Aerosol Generation and Aerosol Sample Collection

SSA were generated using two aerosol generation approaches: the MART (Santander et al., 2022; Stokes et al., 2013; Trueblood et al., 2019) and breaking waves in the waveflume at SIO (Wang et al., 2015). Briefly, the MART uses a periodic plunging waterfall to generate bubble plumes that burst to form SSA. By creating an isolated system for studying SSA, the MART prevents the inclusion of atmospheric aerosols from non-marine sources. The MART has been shown to produce SSA size distributions that are similar to the size distributions measured of nascent SSA in field studies (Stokes et al., 2013). For experiments in the 3,000 L outdoor tank, 100 L of seawater was transferred daily from the outdoor tank to the MARTs and then transferred back to the outdoor tank the following day after refilling the MARTs with a fresh batch of seawater from the outdoor tank (Trueblood et al., 2019). The SIO waveflume is a 33 m long sealed glass channel that uses a moving paddle to create a wave that breaks on an artificial beach, generating SSA (Stokes et al., 2013). Similar to the MART, the waveflume is an isolated system that removes non-marine aerosols.

Aerosols were collected using one of two different methods (see details in Table 1). Aerosols were collected using glass impingers (Chemglass, CG-1820, 0.2 μ m D_p lower cutoff at 1 LPM) containing 20 mL of ultrapure (Type 1) water. The airflow through the impingers was set at 1 LPM for 2 hr for MART experiments and 6 hr for waveflume experiments. Alternatively, aerosols were collected daily using two liquid spot samplers (Aerosol

Devices, LSS110A), which use a condensation growth tube to collect particles (Fernandez et al., 2014), in a size range of 5 nm to $>10\text{ }\mu\text{m}$, into a 0.7 mL liquid vial filled with ultrapure (Type 1) water. The airflow through the spot samplers was 1.5 LPM over the 1 hr collection period. The samples from the two liquid spot samplers were then combined and diluted to 1.5 mL before measuring with EEM spectroscopy.

2.3. Bulk Seawater Collection, DOC, and Microbiology Analysis

Bulk seawater samples were collected and analyzed for EEMs, DOC concentrations, heterotrophic bacteria and virus concentrations, and enzyme activity. All bulk seawater samples were collected in glass vials prepared for total organic carbon analysis. Briefly, vials were cleaned with an acetone rinse followed by several ultrapure water rinses followed by an acid wash with 0.1 N HCl and multiple ultrapure water rinses, then heated at 500°C for 7 hr. Bulk samples were collected daily from a spigot located on the side of the MART or syphoned out of the wave-flume. DOC samples were prepared by filtering seawater with a combusted 0.7 μm glass fiber filter (Whatman GF/F, Z242489) and acidifying to pH 2 with ~ 2 drops of trace metal-free concentrated 12 M HCl. Samples were stored in the dark at room temperature. DOC was analyzed by using the high-temperature combustion method (Shimadzu Instruments) (Alvarez-Salgado & Miller, 1998).

Heterotrophic bacteria and virus concentrations for all experiments were obtained either by epifluorescence microscopy or flow cytometry. All water samples for microbial abundance were preserved using 10% electron microscopy grade glutaraldehyde and then incubated at 4°C for 10 min followed by flash freezing in liquid nitrogen and then storing at -80°C . Samples were analyzed with an epifluorescence microscope (Keyence BZ-X700, final magnification 100X after staining) with SYBR Green I (Life Technologies, S-7563) following the Noble and Furhman protocol for bacteria and viruses (Noble & Fuhrman, 1998). Samples analyzed via flow cytometry (BIO-RAD, ZE5 Cell Analyzer, at The Scripps Research Institute (TSRI) Flow Core Facility) for heterotrophic bacteria were first diluted (1:10) in 1 \times TE buffer (pH 8), then were stained with SYBR Green I at RT for 10 min (at a 10:4 dilution of the commercial stock) in the dark (Gasol & Del Giorgio, 2000). For viruses, samples were diluted (1:50) in 1 \times TE buffer (pH 8) and stained with SYBR Green I at 80°C for 10 min in the dark (at a 5×10^{-5} dilution of the commercial stock). Heterotrophic bacteria and virus populations were discriminated based on their signature in the FL1 (488 nm laser, green fluorescence) versus side scattering (SSC) specific cytograms (Brussaard, 2004; Marie et al., 1997).

Bacterial enzymatic activities (protease, lipase and alkaline phosphatase) were measured using the fluorogenic substrate method (Hoppe, 1983). Briefly, fluorogenic substrates: L-leucine-7-amido-4-methyl-coumarin (Sigma, L2145), 4-methyl-umbelliferyl oleate (Sigma, 75164), 4-methyl-umbelliferyl-phosphate (Sigma, M8883) were added to the sample at 20 μM final concentrations (in Exp1, Exp3, and Exp4). Fluorescence was measured once immediately after the addition of the fluorogenic substrates, incubated in the dark for 45 min, and measured again. Fluorescence was measured using 355 nm excitation and 460 nm emission by a multimode reader (SynergyTM H1, BioTek) on 96-well microliter plates. The fluorescence signal results from the cleavage of free fluorophores (4-methylumbelliflone (MUF) and 7-amido-4-methylcoumarin (AMC)) from the substrate and is directly proportional to the hydrolysis rate and thus the bacterial enzymatic activity. Standard curves were generated for each measurement to relate fluorescence intensity to fluorophore concentration.

Bulk seawater samples were size-fractionated (see Table 1). Seawater was filtered by 0.2 μm filter either with a microanalysis vacuum filter setup (EMD Millipore Corp, Cat. Num. XA5002501) with hand pump (Fisher Scientific, Part Num. 1367811E) and a 0.2 μm polycarbonate filter (EMD Millipore Corp, GTTP02500), or by syringe filtration (BD, 309604; Pall Acrodisc, PN4602). For Exp3 and Exp4, samples were then sequentially filtered via centrifuge filtration using a 50 kDa centrifuge filter (Amicon Ultra 2 mL, UFC205024) and centrifuging at 4,000 g for 15 min (Eppendorf, 5810, Rotor A-4-44). All filtration glassware was cleaned by rinsing with ultrapure water and heating to 500°C for 7 hr. Syringe filters and centrifuge filters were cleaned with several ultrapure water filtrations prior to use.

2.4. Excitation-Emission Matrix Spectroscopy

EEMs were obtained for all bulk seawater and SSA samples using a spectrofluorometer (Horiba Scientific, Aqualog with extended range). Excitation wavelengths ranged from 235 to 450 nm. Emission wavelengths ranged from 250 to 800 nm. A background spectrum was acquired with ultrapure water and subtracted from all EEMs.

EEMs were corrected for inner-filter effects based on absorbance spectra measured simultaneously. Rayleigh scatter (first and second order) was removed. EEMs were also normalized to the area of the Raman Scattering peak of water at 350 nm excitation to convert fluorescence intensities to Raman Units (R.U.) (Lawaetz & Stedmon, 2009; Murphy, 2011). The abundance of HULIS is presented as the fluorescence intensity of the HULIS peak at wavelengths of 360 nm excitation and 450 nm emission unless otherwise specified. All error bars shown for HULIS, unless otherwise noted, represent the standard deviation of the mean ($N = 9$) for the 9 SSA measurements in Exp5 and ($N = 3$) for the 3 SSA measurements in all other experiments.

Four fluorescence indices were calculated to examine changes in HULIS chemical composition. A humification index (here referred to as HIX 1), described by Kalbitz et al. (2000), has been correlated with polycondensation and C/N ratio and is calculated here using the ratio: (intensity at 390 nm excitation/408 nm emission)/(intensity 355 nm excitation/373 emission). A second humification index (here referred to as HIX 2), described by Zsolnay et al. (1999) and Ohno (2002), has been previously used to measure the degree of humification for soil extracts. HIX 2 is calculated here using the ratio at 255 nm excitation: (area under 435–480 nm emission)/(area under 300–345 nm + 435–480 nm emission). A biological index (BIX), first described by Parlanti et al. (2000), has been used to measure the proportion of recently produced DOM and is calculated using the ratio at 310 nm excitation: (intensity at 380 nm emission)/(max intensity between 420 and 435 nm emission). A fluorescence index (FI), described by Cory and McKnight (Cory & McKnight, 2005), has been used to identify the origin of DOM as either microbial or terrestrial and is calculated using the ratio at 370 nm excitation: (intensity at 470 nm emission)/(intensity at 520 nm emission).

3. Results and Discussion

3.1. Microbial Activities Affect HULIS Production in Seawater

Phytoplankton bloom experiments were carried out to investigate differences in HULIS production over a wide range of biological conditions and different bloom densities. The progression of the phytoplankton blooms were monitored using *in vivo* chlorophyll-a fluorescence, which is used as a proxy for phytoplankton biomass (Figure 1). Each bloom experiment showed similar behavior in terms of a chlorophyll-a increase followed by a decrease over several days, with the exception of Exp7, which showed minimal change in chlorophyll-a levels, representing a non-bloom scenario. Notably, the chlorophyll-a data for Exp1 produced two maxima, indicative of two sequential phytoplankton bloom cycles. All blooms showed very different bloom densities (indicated by chlorophyll-a), with maximum values ranging from 1.90 $\mu\text{g/L}$ (during Exp7) to 39.08 $\mu\text{g/L}$ (in Exp5). The heterotrophic bacteria and virus concentrations peaked approximately 3 days after the peak in chlorophyll-a in most experiments (Figure 1), with the exception of Exp7. This staggered progression is consistent with previous phytoplankton bloom experiments (Lee et al., 2015).

Nutrient additions induced phytoplankton blooms which influenced heterotrophic bacteria and virus abundances in the seawater. EEMs of seawater HULIS reflect the enhanced biological activity. In all cases, the intensity of the HULIS fluorescence peak measured by EEMs increased over time, indicating steady production and accumulation of HULIS in seawater (Figure 1). Even for Exp1 and Exp7, which exhibited distinctive bloom dynamics, accumulation of HULIS occurred over time. Despite the wide range in phytoplankton bloom densities, HULIS accumulation was not correlated with maxima in *in vivo* chlorophyll, suggesting phytoplankton abundance is not singularly responsible for HULIS concentration in seawater (Figure S1 in Supporting Information S1). Therefore, a combination of both phytoplankton and bacteria were responsible for the increased HULIS concentration.

In order to further probe the roles of bacteria and their enzymes on HULIS production, EEMs were collected from phytoplankton bloom experiments with and without the addition of specific marine bacteria isolates to enhance enzyme activity (Exp3 and Exp4, respectively). The enzyme activities for proteases, lipases, and alkaline phosphatases, important for sea-air transfer (Malfatti et al., 2019; Wang et al., 2015), were also monitored over time. While Exp3 and Exp4 began with the same seawater, Exp4 showed enhanced HULIS production after the addition of bacteria isolates compared to Exp3, which did not have bacteria isolates added (Figure 2, Day 4–9). Enzyme activity data showed that the added bacterial strains resulted in high alkaline phosphatase activity (Figure 2), thus leading to a significant change in phosphorous-rich compounds in seawater. These findings support the hypothesis that bacterial enzyme activity enhances the production of HULIS in the seawater.

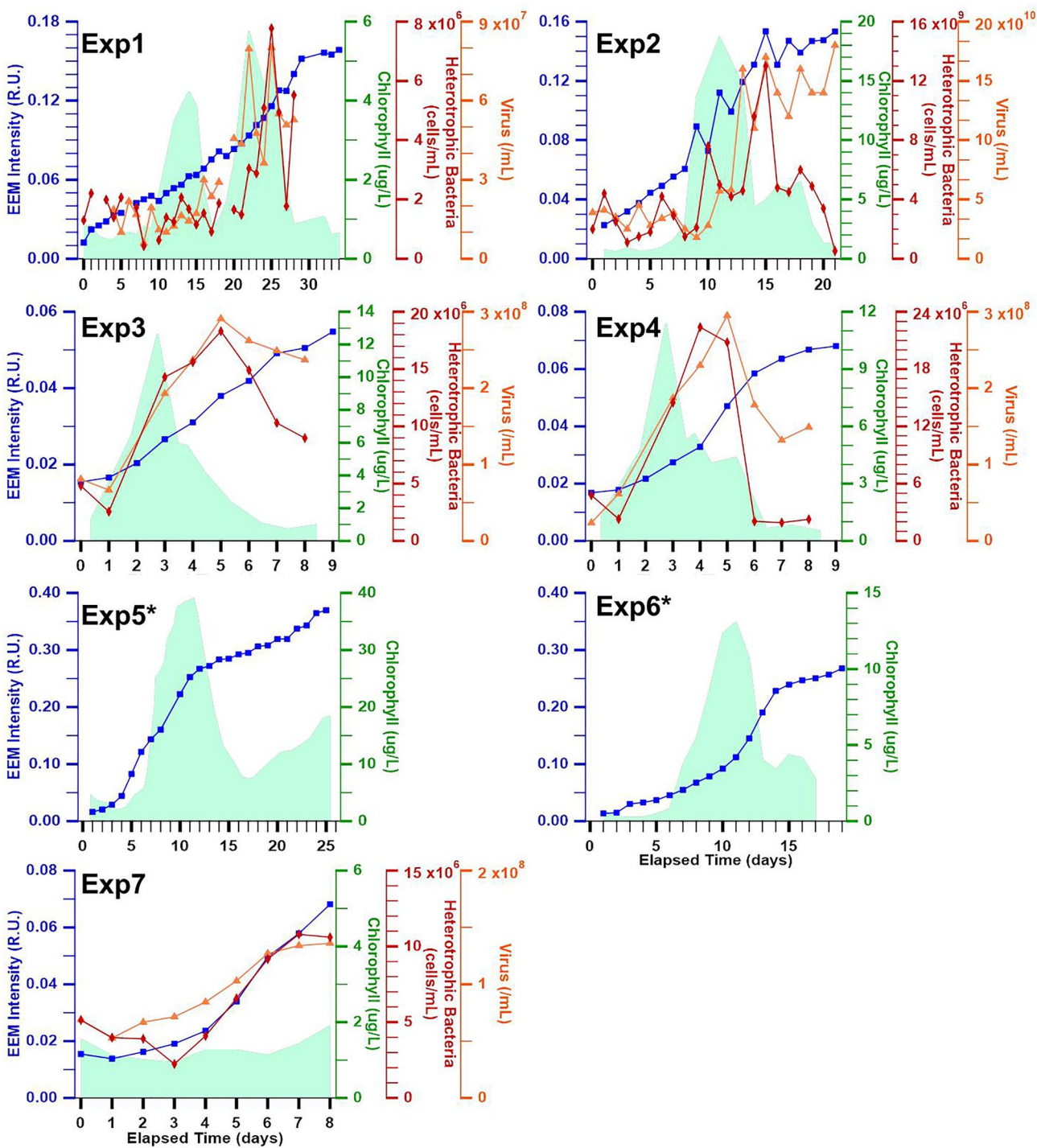


Figure 1. Time series for chlorophyll-a, humic-like substances fluorescence (360 nm excitation, 450 nm emission), heterotrophic bacteria concentrations and virus concentrations in bulk seawater during phytoplankton blooms in seven experiments. Asterisks (*) indicate no measurements for bacterial and viral abundance.

3.2. Seawater HULIS Correlate With DOC and Display a Narrow Size Range

In all experiments, temporal changes in bulk seawater HULIS EEM intensity correlated with DOC (Figure 3, Spearman's ρ ranges from 0.79 to 0.98). This correlation suggests that (a) the organic molecules that make up the DOC pool contribute to HULIS and (b) higher DOC concentrations are associated with higher HULIS fluorescence intensities. Similar correlations have been observed previously (Mostofa et al., 2007). Conventionally,

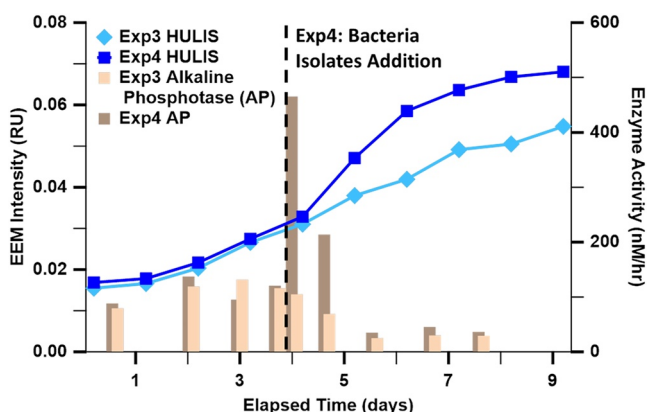


Figure 2. Humic-like substances fluorescence (360 nm excitation, 450 nm emission) over time during Exp3 and Exp4 with alkaline phosphatase activity over time during Exp3 and Exp4. Marine bacteria isolates added to Marine Aerosol Reference Tank in Exp4 on day 4.

humic-like molecules are considered to be very complex, with structures that are often recalcitrant and thus can persist in the environment (Graber & Rudich, 2006). On the other hand, it is known that during enclosed manipulation experiments, DOC tends to accumulate despite bacterial growth, thus becoming less labile and more recalcitrant (Aluwihare & Repeta, 1999; Gruber et al., 2006). Therefore, we speculate that linking DOC and HULIS can provide insight into the degree of recalcitrance of the DOC.

From the analysis of the EEM versus DOC slopes across the entire data set, we distinguish three families of slope steepness: Exp1-like; Exp2-3-4-like and Exp5-6-like (Figure 4). Moreover, we propose that the slope steepness is related to the extent of the chemical modification caused by bacterial enzymatic activities and growth on the DOC pool that influences its recalcitrance (or lability). It is known that marine bacteria can produce slow-to-degrade/recalcitrant DOC (Gruber et al., 2006). Because the slope relates the change in DOC to the change in HULIS, a steeper slope indicates the presence of labile DOC, which is quickly processed by bacteria growth and enzymatic activity to form more recalcitrant molecules, such as HULIS.

When plotting the ratio of DOC/HULIS over time, we notice an exponential decay in all experiments that suggests an increase in HULIS contribution to

the DOC pool (Figure S2 in Supporting Information S1). Higher enzymatic activities were measured in Exp2-3-4 than in family Exp1, suggesting that during Exp2-3-4, the DOC pools were processed more intensively thus depleting the labile compounds faster and creating more recalcitrant molecules that had a stronger HULIS signal intensity (Figure S3 in Supporting Information S1).

To identify size-dependent changes in HULIS concentrations, seawater samples were sequentially filtered (Figure 5). The majority of the HULIS EEM signal (>80%) was in the smallest size fraction (<50 kDa or <0.2 μ m),

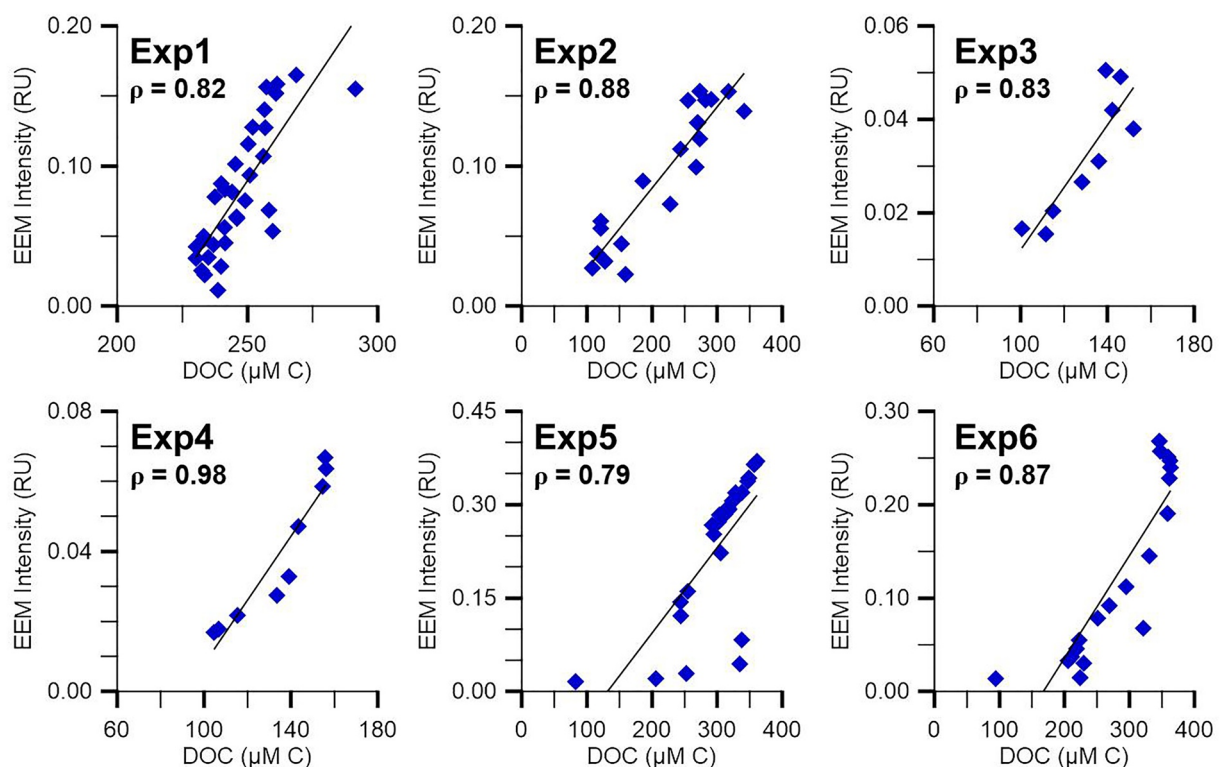


Figure 3. Correlations between humic-like substances excitation emission matrix intensity (360 nm excitation, 450 nm emission) and dissolved organic carbon (DOC) concentrations in bulk seawater for multiple phytoplankton bloom experiments (except for Exp7 where DOC was not sampled). Spearman's correlation coefficient, ρ , listed for each experiment.

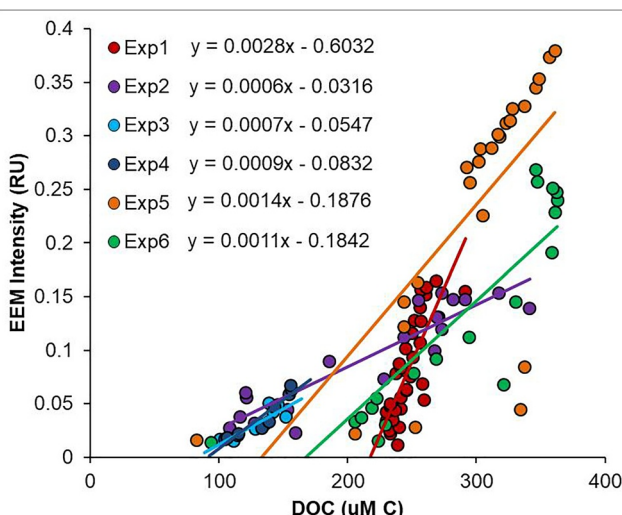


Figure 4. Excitation emission matrix versus dissolved organic carbon (DOC) for all experiments (with points and slopes color coded for each experiment), except for Exp7 where DOC was not sampled.

Kalbitz et al., 2000; Miano et al., 1990; Ohno, 2002; Parlanti et al., 2000; Zsolnay et al., 1999) (Figure 6, Figures S4 and S5 in Supporting Information S1). We monitored the HULIS wavelength shifts in the four experiments in order to test the hypothesis that microbial activities were responsible for changes in HULIS chemistry. Previous work has shown that HULIS fractions with lower fluorescence emission peak (~400 nm) are found to be less oxygenated, while HULIS fractions with higher fluorescence peaks (~450 nm) have been assigned to highly oxygenated species, which can be from photodegradation of less oxygenated organic matters (Barsotti et al., 2016; Chen et al., 2003; Senesi et al., 1991).

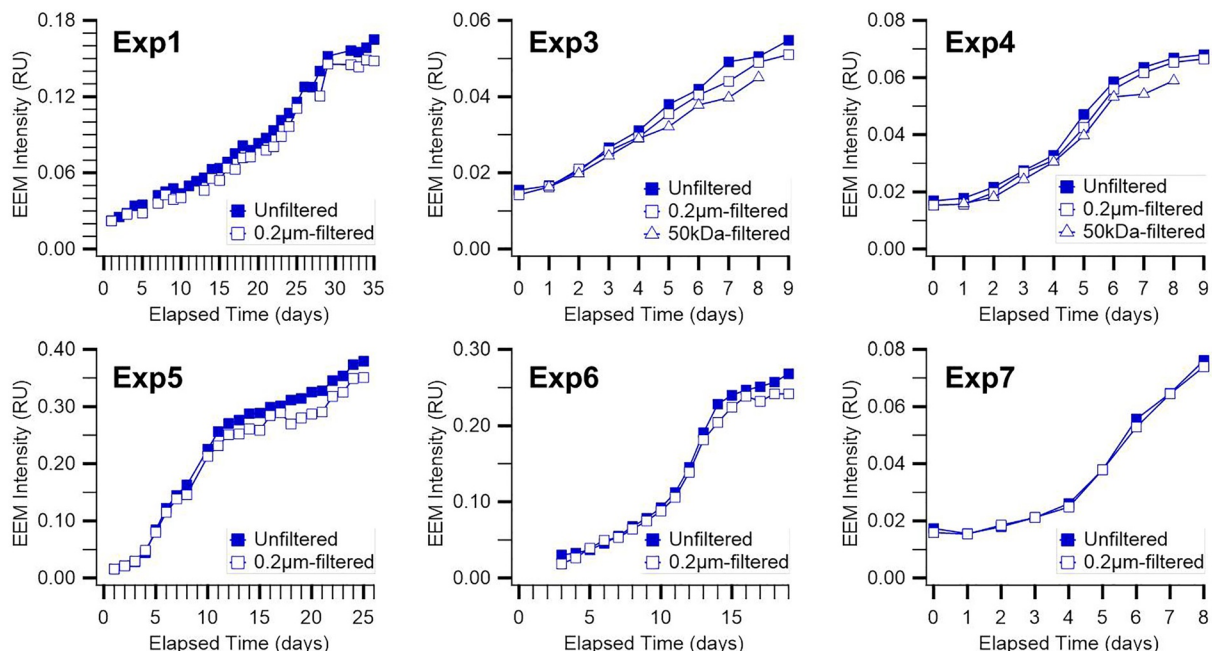


Figure 5. Size fractionation of humic-like substances (HULIS) in seawater: HULIS excitation emission matrix intensity (360 nm excitation, 450 nm emission) before and after initial and subsequent filtrations.

even in experiments with large bloom intensities and high DOC concentrations. Small bacteria (Yang & Nagata, 2021) and viruses (Li & Dickie, 1985; Zimmermann, 1977) will go through the 0.2 µm filter membrane, but given the fact that the 50 kDa cartridge has a nominal size of 5 nm and the retention specification state optimum viral recovery above 15 nm, the signal in the <50 kDa filtrate primarily originated from HULIS. While previous studies have also shown the majority of HULIS to be in the smallest size fractions (Grzybowski, 1995), this study shows that this size-dependence holds throughout a phytoplankton bloom cycle. This result confirms that the majority of the HULIS fluorescent signal does not originate from the bacteria or viruses themselves. The retention of HULIS fluorescence after filtration supports the hypothesis that HULIS in SSA are largely derived from the dissolved fraction of organic matter in the DOC pool.

3.3. Microbial Activities Affect HULIS Chemistry

Following HULIS concentration findings in seawater, we investigated links between bacterial enzyme activity and HULIS chemical composition. Changes in HULIS chemical composition were monitored through shifts in the wavelength at maximum HULIS emission and three different fluorescence indexes: two humification indexes, here referred to as HIX 1 and HIX 2, and a biological index (BIX) (Chen et al., 2003; Cory & McKnight, 2005;

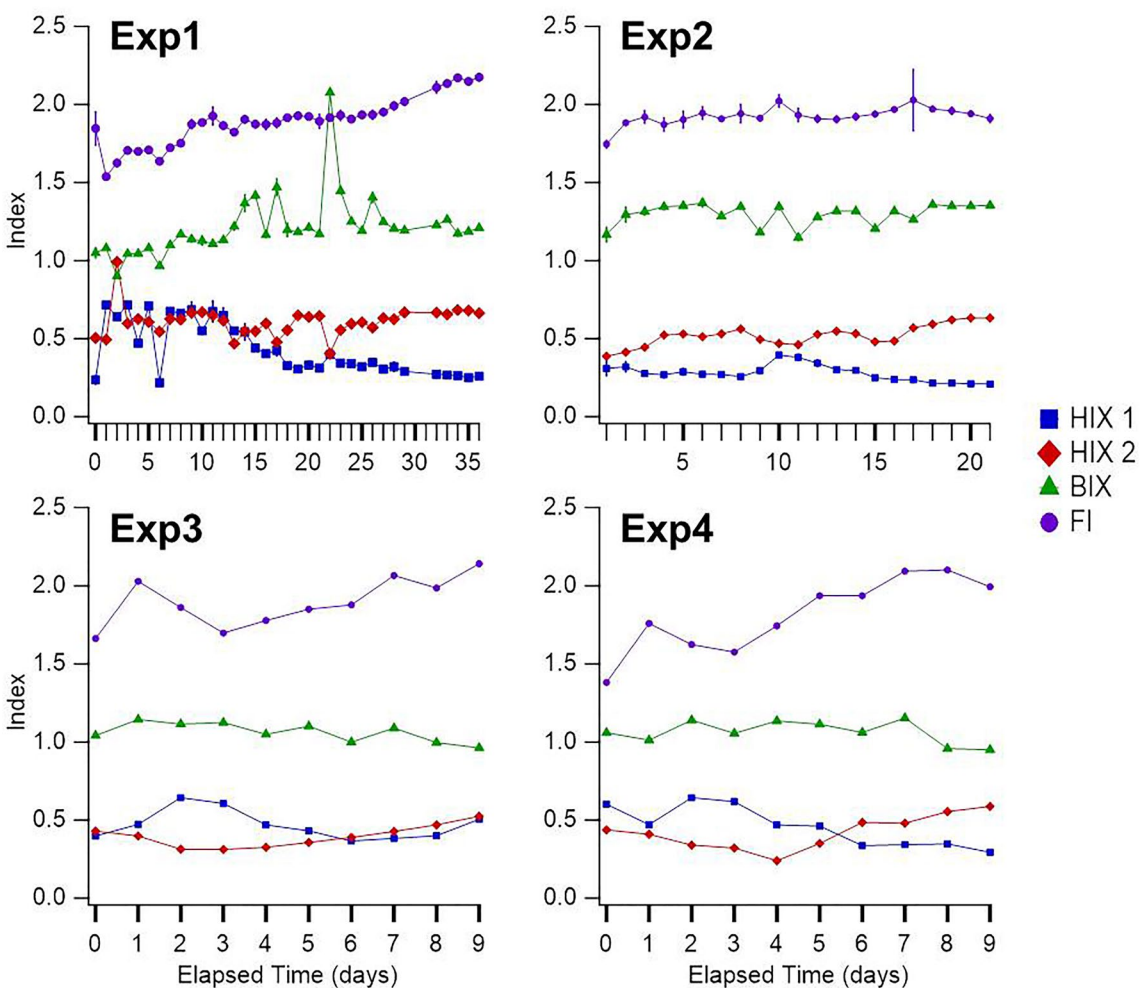


Figure 6. Fluorescence indices (HIX 1, HIX 2, BIX, and fluorescence index) in bulk seawater over time for Exp1-Exp4. Lines shown for Exp1-Exp2 represent one standard deviation and are often smaller than the marker size.

In Exp1, we observed a small shift in the HULIS emission maximum for filtered bulk seawater from 426 nm near the beginning of the experiment to 450 nm leading into the first phytoplankton bloom peak (Figure S4 in Supporting Information S1). The HULIS emission maximum during the second bloom showed an even smaller shift compared to the first bloom, likely due to the formation of already-processed, recalcitrant material that is resistant to further enzymatic breakdown. A shift was also observed in Exp2 during the last 5 days of the experiment. In Exp3 and Exp4, the maximum of the HULIS EEM signal shifted from 445 nm at the beginning of the bloom to 455 nm near the peak of the bloom, followed by a shift back to 445 nm several days later (Figure S4 in Supporting Information S1). These shifts indicated that the HULIS chemical composition changed over the course of a phytoplankton bloom.

Fluorescence indices over time also indicate changing HULIS chemical composition (Figure 6, Figure S5 in Supporting Information S1). FI was increasing during the experiments suggesting greater contribution of microbial reworking of DOM-HULIS. In Exp1 and Exp2, BIX showed an increase in more freshly produced DOM over time. In Exp3 and Exp4, BIX presented minimal changes suggesting an equilibrium between fresh production and aging. HIX 1 presented a maximum in every experiment that then decreased thus indicating less polycondensation and higher C/N ratio. HIX 2 showed an increase in every experiment, suggesting greater degree of humification over time.

Comparing the enzyme activities with the shifts in fluorescence emission and the fluorescence indices suggests that bacteria drive the changes in HULIS chemical composition. Shifts in the wavelength at maximum HULIS

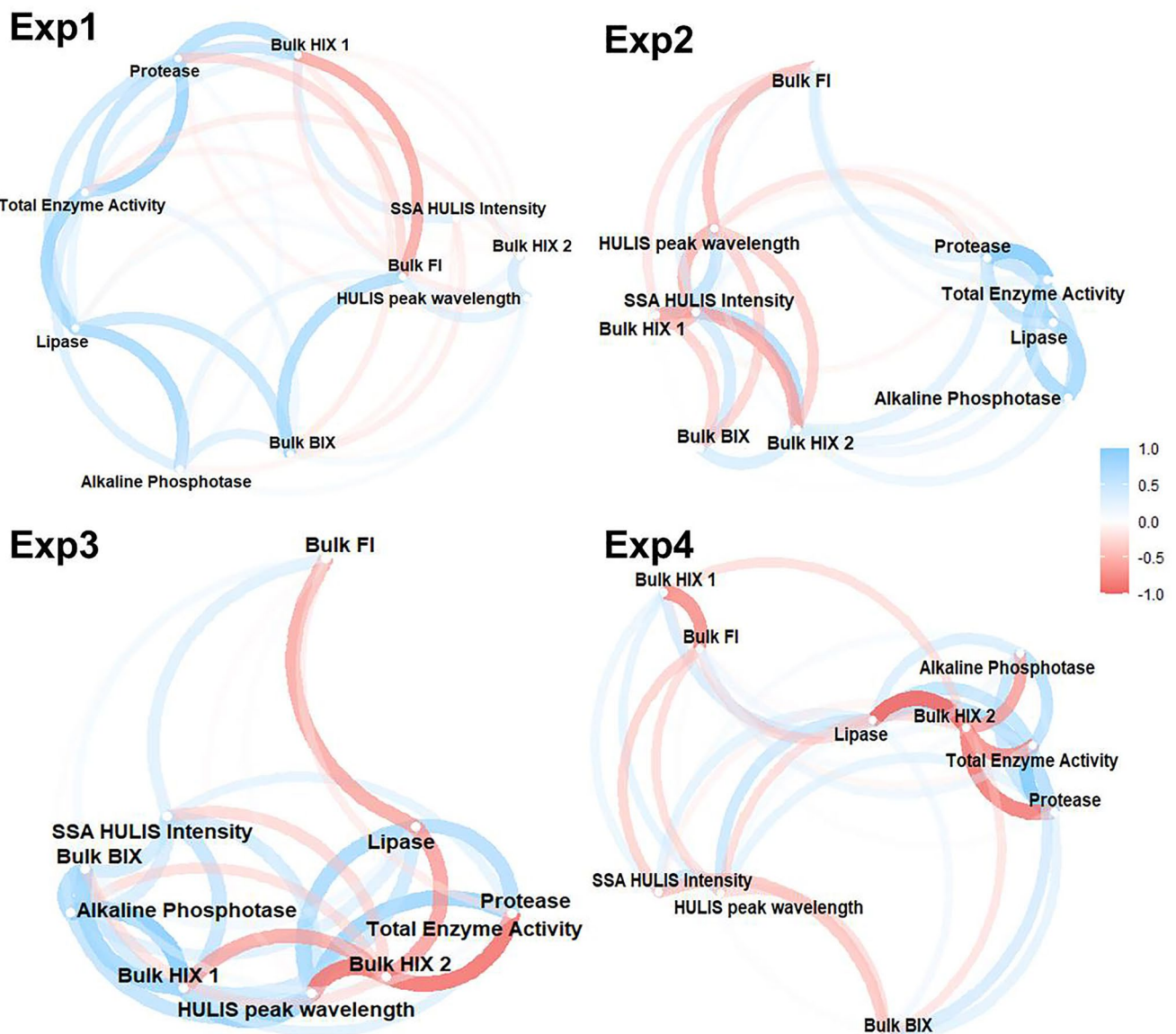


Figure 7. Correlation network plots for Exp1, 2, 3, 4 with the following variables: sea spray aerosols humic-like substances (HULIS) intensity, HULIS peak wavelength, total enzyme activities, proteases, lipases, alkaline phosphatases, bulk seawater HIX 1, bulk seawater HIX 2, bulk BIX, and bulk fluorescence index. Blue indicates positive correlation. Red indicates negative correlation.

emission were contemporaneous with the changes in enzymatic activities (Figure 7). In Exp1 and Exp2, changes in HULIS chemistry were driven by proteases and lipases, while in Exp3 and Exp4, HULIS chemistry were driven by bacterial alkaline phosphatases (Figure 7, Figure S4 in Supporting Information S1). For fluorescence indices, lipase activity was correlated with HIX 1 and BIX in three out of four experiments. Moreover, these experiments showed strong correlations between proteases and HIX 2. Future experiments could further explore the link between enzymes and fluorescence indices by identifying the fatty acid and amino acid fingerprints during incubation experiments. The correspondence between enzyme activity and HULIS composition in the seawater. These changes likely impact the efficiency of air-sea transfer (Malfatti et al., 2019; Wang et al., 2015).

3.4. HULIS Transfer From the Ocean to the Atmosphere

We show that bacteria enzymatic activities are associated with HULIS production in seawater, and that HULIS chemical composition can change over the course of a bloom. To assess how these seawater changes impact the sea-air transfer of HULIS, SSA samples collected during Exp1-Exp7 were analyzed for changes in HULIS concentrations over the course of phytoplankton blooms. The “transmission factor” (defined here as the ratio of the maximum HULIS intensity in bulk seawater to the maximum HULIS intensity in SSA) is on the order of 10^3 – 10^4 (with a range of 1,300–14,000) and is comparable across experiments. As mentioned previously, bulk seawater EEMs consistently showed an increase in HULIS over the course of a phytoplankton bloom. For SSA, however, despite the steady accumulation of HULIS in bulk seawater, HULIS enrichment in SSA did not follow the same trend. In contrast, SSA HULIS concentrations rose and fell throughout a bloom, rather than increasing steadily as observed in seawater (Figure 8).

Comparing HULIS in SSA with HULIS chemical composition data indicated through emission wavelength shifts and fluorescence indices suggest that changes in HULIS chemical composition drive the transfer of HULIS from seawater to SSA (Figure 7, Figure S6 in Supporting Information S1). In three out of four experiments, SSA HULIS intensity positively correlated with bulk HIX 1. Three experiments also showed strong correlations between SSA HULIS and BIX, suggesting that transfer may be associated with DOM aging. The links between SSA HULIS and bulk seawater HULIS chemistry are consistent with the correlations observed between HULIS chemistry and enzyme activity (Figure 7) mentioned previously. These findings are also consistent with previous work showing that enzymes influence SSA organic matter (Wang et al., 2015). Thus, the combination of high enzyme activities, the changes in HULIS chemical composition, and HULIS dynamics in SSA suggests that enzyme activity regulates HULIS sea-air transfer by transforming HULIS chemical composition to diverse structures. The specific structures that lead to enhanced HULIS in SSA require further studies. Alternatively high enzyme activities at the sea surface could influence the interface properties (e.g., the packing of molecules at the interface (Shrestha et al., 2018), the molecular features of the sea surface microlayer, or the surface adsorption (Cochran et al., 2016)) and thus the ability to release HULIS in SSA. Microbial activity plays a central role in transforming seawater composition (Wang et al., 2015), leading to the transfer of HULIS from bulk seawater to SSA.

4. Conclusion

This study aims to elucidate the biological factors controlling the dynamics of HULIS and transfer from the ocean to the atmosphere under a range of ocean microbiological conditions. Specifically, the influence of marine bacteria and their enzymes on HULIS size, production, and chemical composition were investigated to elucidate the effects that influence sea-air transfer. Regarding HULIS size over the course of each phytoplankton bloom, seawater HULIS concentration consistently increased over the course of the bloom and correlated with DOC; however, throughout the entire bloom progression, the vast majority of HULIS existed in the smallest seawater size fraction (<50 kDa). For HULIS production, perturbation experiments with marine bacteria isolates additions revealed that bacteria and their enzymes enhanced the production and increased concentrations of HULIS. Finally, fluorescence indices and shifts in the HULIS emission spectra correlated with enzyme activities, suggesting that marine bacteria induce changes in HULIS chemical composition through enzymatic activity.

In this study, we hypothesized that bacteria drive changes in HULIS size, production, and chemical composition, and that these changes induced by bacteria enhance the transfer of HULIS to SSA. In the quest to elucidate the impact of enzymes on HULIS sea-air transfer, we note that changes in SSA HULIS did not correlate with chlorophyll-a, DOC, heterotrophic bacteria, or virus concentrations. Our findings suggest that the changes in HULIS chemical composition, induced by bacterial enzymes, are the major drivers for the sea-air transfer of HULIS. While bacteria do play a role in affecting HULIS size and production, these factors appear to be less vital for sea-air transfer than the induced changes in chemical composition. Thus, we provide evidence that bacterial enzymatic activities drive changes in seawater chemistry, which then directly impact SSA chemical composition. This study emphasizes the complex role that marine microorganisms, specifically bacterial enzymatic activity, play in SSA formation and composition.

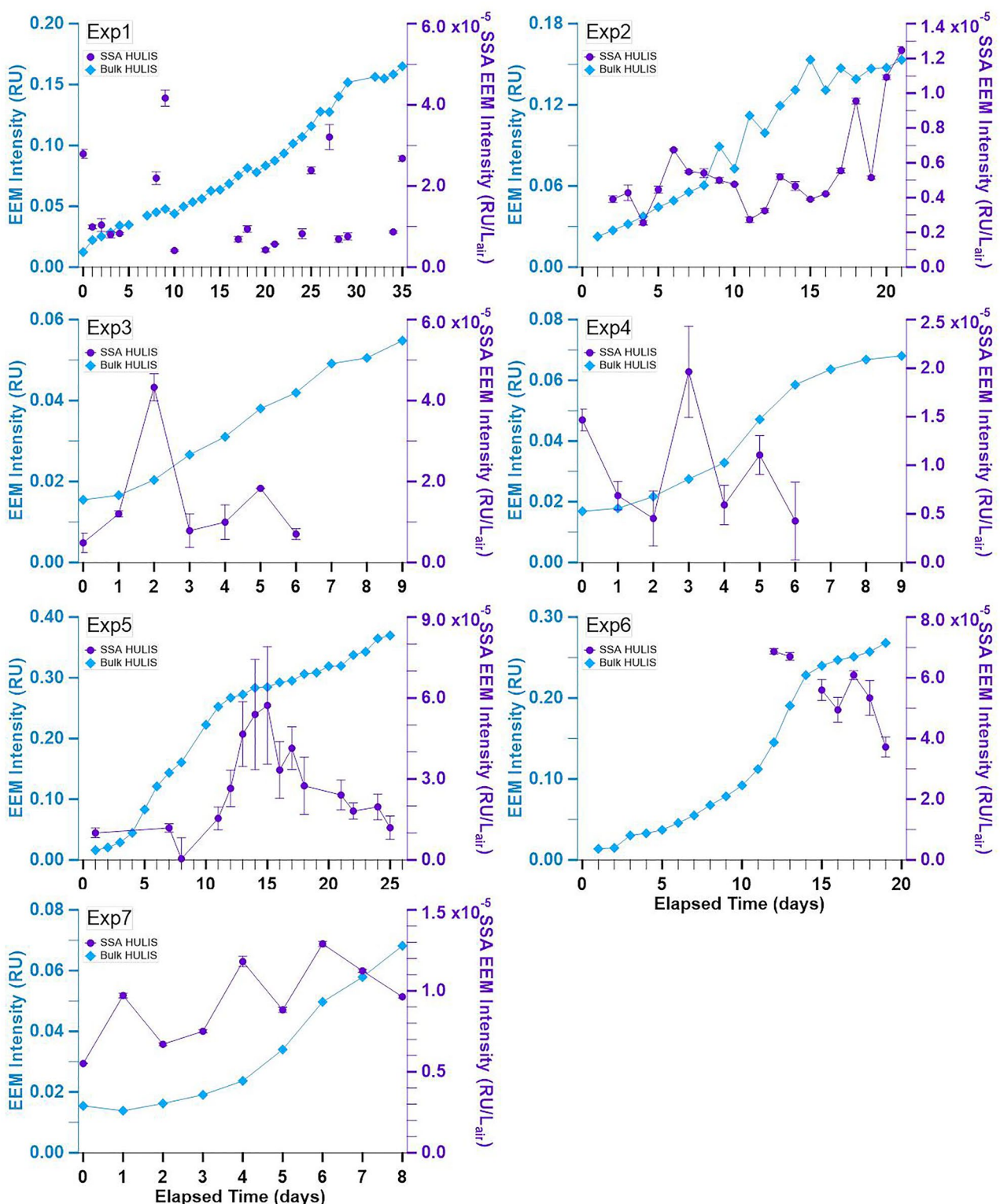


Figure 8. Humic-like substances excitation emission matrix intensity in seawater (blue) and sea spray aerosols (purple) over the course of various induced phytoplankton bloom experiments. Error bars represent the standard deviation of the mean ($N = 9$ for Exp5, $N = 3$ for all other experiments).

Data Availability Statement

All data supporting the conclusions in this study are publicly available at: <https://doi.org/10.6075/J0S46S4J>.

Acknowledgments

The authors would like to thank Julie Dinasquet and Rebecca Simpson for valuable discussion and feedback. This work was funded by the National Science Foundation Center for Aerosol Impacts on the Chemistry of the Environment (NSF-CAICE), a Center for Chemical Innovation (CHE-1801971).

References

Aluwihare, L. I., & Repeta, D. J. (1999). A comparison of the chemical characteristics of oceanic DOM and extracellular DOM produced by marine algae. *Marine Ecology Progress Series*, 186, 105–117. <https://doi.org/10.3354/Meps186105>

Alvarez-Salgado, X. A., & Miller, A. E. J. (1998). Simultaneous determination of dissolved organic carbon and total dissolved nitrogen in seawater by high temperature catalytic oxidation: Conditions for precise shipboard measurements. *Marine Chemistry*, 62(3–4), 325–333. [https://doi.org/10.1016/S0304-4203\(98\)00037-1](https://doi.org/10.1016/S0304-4203(98)00037-1)

Azam, F., Fenchel, T., Field, J. G., Gray, J. S., Meyer-Reil, L. A., & Thingstad, F. (1983). The ecological role of water-column microbes in the sea. *Marine Ecology Progress Series*, 10(3), 257–263. <https://doi.org/10.3354/meps01025>

Barsotti, F., Ghigo, G., & Vione, D. (2016). Computational assessment of the fluorescence emission of phenol oligomers: A possible insight into the fluorescence properties of humic-like substances (HULIS). *Journal of Photochemistry and Photobiology A: Chemistry*, 315, 87–93. <https://doi.org/10.1016/j.jphotochem.2015.09.012>

Bidle, K. D., & Azam, F. (2001). Bacterial control of silicon regeneration from diatom detritus: Significance of bacterial ectohydrolases and species identity. *Limnology & Oceanography*, 46(7), 1606–1623. <https://doi.org/10.4319/lo.2001.46.7.1606>

Borgatta, J., & Navea, J. G. (2015). Fate of aqueous iron leached from tropospheric aerosols during atmospheric acidic processing: A study of the effect of humic-like substances. *Air Pollution XXIII*, 198, 155–166. <https://doi.org/10.2495/Air150131>

Brown, T. E., & Richards, F. L. (1968). Effect of growth environment on physiology of algae - Light intensity. *Journal of Phycology*, 4(1), 38–54. <https://doi.org/10.1111/j.1529-8817.1968.tb04675.x>

Brussaard, C. P. D. (2004). Optimization of procedures for counting viruses by flow cytometry. *Applied and Environmental Microbiology*, 70(3), 1506–1513. <https://doi.org/10.1128/Aem.70.3.1506-1513.2004>

Cavalli, F., Facchini, M. C., De Cesari, S., Mircea, M., Emblico, L., Fuzzi, S., & Dell'Acqua, A. (2004). Advances in characterization of size-resolved organic matter in marine aerosol over the North Atlantic. *Journal of Geophysical Research*, 109(D24), D24215. <https://doi.org/10.1029/2004jd005137>

Chen, J., LeBoef, E. J., Dai, S., & Gu, B. H. (2003). Fluorescence spectroscopic studies of natural organic matter fractions. *Chemosphere*, 50(5), 639–647. [https://doi.org/10.1016/S0045-6535\(02\)00616-1](https://doi.org/10.1016/S0045-6535(02)00616-1)

Chen, J., Wu, Z. J., Zhao, X., Wang, Y. J., Chen, J. C., Qiu, Y. T., et al. (2021). Atmospheric humic-like substances (HULIS) act as ice active entities. *Geophysical Research Letters*, 48(14). <https://doi.org/10.1029/2021GL092443>

Coble, P. G. (2007). Marine optical biogeochemistry: The chemistry of ocean color. *Chemical Reviews*, 107(2), 402–418. <https://doi.org/10.1021/cr050350+>

Cochran, R. E., Jayathathne, T., Stone, E. A., & Grassian, V. H. (2016). Selectivity across the interface: A test of surface activity in the composition of organic-enriched aerosols from bubble bursting. *Journal of Physical Chemistry Letters*, 7(9), 1692–1696. <https://doi.org/10.1021/acs.jpclett.6b00489>

Cory, R. M., & McKnight, D. M. (2005). Fluorescence spectroscopy reveals ubiquitous presence of oxidized and reduced quinones in dissolved organic matter. *Environmental Science & Technology*, 39(21), 8142–8149. <https://doi.org/10.1021/es0506962>

Fernandez, A. E., Lewis, G. S., & Hering, S. V. (2014). Design and laboratory evaluation of a sequential spot sampler for time-resolved measurement of airborne particle composition. *Aerosol Science and Technology*, 48(6), 655–663. <https://doi.org/10.1080/02786826.2014.911409>

Freney, E., Sellegrí, K., Nicosia, A., Williams, L. R., Rinaldi, M., Trueblood, J. T., et al. (2021). Mediterranean nascent sea spray organic aerosol and relationships with seawater biogeochemistry. *Atmospheric Chemistry and Physics*, 21(13), 10625–10641. <https://doi.org/10.5194/acp-21-10625-2021>

Gasol, J. M., & Del Giorgio, P. A. (2000). Using flow cytometry for counting natural planktonic bacteria and understanding the structure of planktonic bacterial communities. *Scientia Marina*, 64(2), 197–224. <https://doi.org/10.3989/scimar.2000.64n2197>

Graber, E. R., & Rudich, Y. (2006). Atmospheric HULIS: How humic-like are they? A comprehensive and critical review. *Atmospheric Chemistry and Physics*, 6(3), 729–753. <https://doi.org/10.5194/acp-6-729-2006>

Gruber, D. F., Simjouw, J. P., Seitzinger, S. P., & Taghon, G. L. (2006). Dynamics and characterization of refractory dissolved organic matter produced by a pure bacterial culture in an experimental predator-prey system. *Applied and Environmental Microbiology*, 72(6), 4184–4191. <https://doi.org/10.1128/Aem.02882-05>

Grzybowski, W. (1995). Selected properties of different molecular size fractions of humic substances isolated from surface Baltic water in the Gdansk Deep area. *Oceanologia*, 38(1), 33–47.

Guillard, R. R., & Ryther, J. H. (1962). Studies of marine planktonic diatoms. I. Cyclotella nana Hustedt, and Detonula confervacea (Cleve) Gran. *Canadian Journal of Microbiology*, 8(2), 229–239. <https://doi.org/10.1139/m62-029>

Hessen, D. O., & Tranvik, L. J. (1998). *Aquatic humic substances: Ecology and biogeochemistry*. Springer.

Hoppe, H. G. (1983). Significance of exoenzymatic activities in the ecology of brackish water: Measurements by means of methylumbelliferyl-substrates. *Marine Ecology Progress Series*, 11(3), 299–308. <https://doi.org/10.3354/Meps01129>

Kalbitz, K., Geyer, S., & Geyer, W. (2000). A comparative characterization of dissolved organic matter by means of original aqueous samples and isolated humic substances. *Chemosphere*, 40(12), 1305–1312. [https://doi.org/10.1016/S0045-6535\(99\)00238-6](https://doi.org/10.1016/S0045-6535(99)00238-6)

Lawaetz, A. J., & Stedmon, C. A. (2009). Fluorescence intensity calibration using the Raman scatter peak of water. *Applied Spectroscopy*, 63(8), 936–940. <https://doi.org/10.1366/000370209788964548>

Lee, C., Sultana, C. M., Collins, D. B., Santander, M. V., Axson, J. L., Malfatti, F., et al. (2015). Advancing model systems for fundamental laboratory studies of sea spray aerosol using the microbial loop. *Journal of Physical Chemistry A*, 119(33), 8860–8870. <https://doi.org/10.1021/acs.jpca.5b03488>

Li, W., & Dickie, P. (1985). Growth of bacteria in seawater filtered through 0.2 µm nucleopore membranes: Implications for dilution experiments. *Marine Ecology Progress Series*, 26, 245–252. <https://doi.org/10.3354/meps026245>

Malfatti, F., Lee, C., Tinta, T., Pendergraft, M. A., Celussi, M., Zhou, Y. Y., et al. (2019). Detection of active microbial enzymes in nascent sea spray aerosol: Implications for atmospheric chemistry and climate. *Environmental Science and Technology Letters*, 6(3), 171–177. <https://doi.org/10.1021/acs.estlett.8b00699>

Marie, D., Partensky, F., Jacquet, S., & Vaulot, D. (1997). Enumeration and cell cycle analysis of natural populations of marine picoplankton by flow cytometry using the nucleic acid stain SYBR Green I. *Applied and Environmental Microbiology*, 63(1), 186–193. <https://doi.org/10.1128/aem.63.1.186-193.1997>

Miano, T., Sposito, G., & Martin, J. P. (1990). Fluorescence spectroscopy of model humic acid-type polymers. *Geoderma*, 47(3–4), 349–359. [https://doi.org/10.1016/0016-7061\(90\)90038-B](https://doi.org/10.1016/0016-7061(90)90038-B)

Mostofa, K. M. G. (2013). *Photobiogeochemistry of organic matter: Principles and practices in water environments*. Springer.

Mostofa, K. M. G., Yoshioka, T., Konohira, E., & Tanoue, E. (2007). Photodegradation of fluorescent dissolved organic matter in river waters. *Geochemical Journal*, 41(5), 323–331. <https://doi.org/10.2343/geochemj.41.323>

Murphy, K. R. (2011). A note on determining the extent of the water Raman peak in fluorescence spectroscopy. *Applied Spectroscopy*, 65(2), 233–236. <https://doi.org/10.1366/10-06136>

Murphy, K. R., Stedmon, C. A., Graeber, D., & Bro, R. (2013). Fluorescence spectroscopy and multi-way techniques. PARAFAC. *Analytical Methods*, 5(23), 6557. <https://doi.org/10.1039/c3ay41160e>

Nebbiosi, A., & Piccolo, A. (2013). Molecular characterization of dissolved organic matter (DOM): A critical review. *Analytical and Bioanalytical Chemistry*, 405(1), 109–124. <https://doi.org/10.1007/s00216-012-6363-2>

Noble, R. T., & Fuhrman, J. A. (1998). Use of SYBR Green I for rapid epifluorescence counts of marine viruses and bacteria. *Aquatic Microbial Ecology*, 14(2), 113–118. <https://doi.org/10.3354/ame014113>

O'Dowd, C., Ceburnis, D., Ovadnevaite, J., Bialek, J., Stengel, D. B., Zacharias, M., et al. (2015). Connecting marine productivity to sea-spray via nanoscale biological processes: Phytoplankton dance or death disco? *Scientific Reports*, 5(1), 14883. <https://doi.org/10.1038/srep14883>

Ohno, T. (2002). Fluorescence inner-filtering correction for determining the humification index of dissolved organic matter. *Environmental Science & Technology*, 36(4), 742–746. <https://doi.org/10.1021/es0155276>

Parlanti, E., Worz, K., Geoffroy, L., & Lamotte, M. (2000). Dissolved organic matter fluorescence spectroscopy as a tool to estimate biological activity in a coastal zone submitted to anthropogenic inputs. *Organic Geochemistry*, 31(12), 1765–1781. [https://doi.org/10.1016/S0146-6380\(00\)00124-8](https://doi.org/10.1016/S0146-6380(00)00124-8)

Pedler, B. E., Aluwihare, L. I., & Azam, F. (2014). Single bacterial strain capable of significant contribution to carbon cycling in the surface ocean. *Proceedings of the National Academy of Sciences of the United States of America*, 111(20), 7202–7207. <https://doi.org/10.1073/pnas.1401887111>

Pohlker, C., Huffman, J. A., & Poschl, U. (2012). Autofluorescence of atmospheric bioaerosols – Fluorescent biomolecules and potential interferences. *Atmospheric Measurement Techniques*, 5(1), 37–71. <https://doi.org/10.5194/amt-5-37-2012>

Prather, K. A., Bertram, T. H., Grassian, V. H., Deane, G. B., Stokes, M. D., DeMott, P. J., et al. (2013). Bringing the ocean into the laboratory to probe the chemical complexity of sea spray aerosol. *Proceedings of the National Academy of Sciences of the United States of America*, 110(19), 7550–7555. <https://doi.org/10.1073/pnas.1300262110>

Rashid, M. A. (1985). *Geochemistry of marine humic compounds*. Springer-Verlag.

Sambrook, J., Fritsch, E. F., & Maniatis, T. (1989). *Molecular cloning: A laboratory manual*. Cold Spring Harbor Laboratory.

Santander, M. V., Schiffer, J. M., Lee, C., Axson, J. L., Tauber, M. J., & Prather, K. A. (2022). Factors controlling the transfer of biogenic organic species from seawater to sea spray aerosol. *Scientific Reports*, 12(1), 3580. <https://doi.org/10.1038/s41598-022-07335-9>

Sauer, J. S., Mayer, K. J., Lee, C., Alves, M. R., Amiri, S., Bahaveolos, C. J., et al. (2022). The Sea Spray Chemistry and Particle Evolution study (SeaSCAPE): Overview and experimental methods. *Environmental Science-Processes & Impacts*, 24(2), 290–315. <https://doi.org/10.1039/d1em00260k>

Senesi, N., Miano, T. M., Provenzano, M. R., & Brunetti, G. (1991). Characterization, differentiation, and classification of humic substances by fluorescence spectroscopy. *Soil Science*, 152(4), 259–271. <https://doi.org/10.1097/00010694-199110000-00004>

Shrestha, M., Luo, M., Li, Y. M., Xiang, B., Xiong, W., & Grassian, V. H. (2018). Let there be light: Stability of palmitic acid monolayers at the air/salt water interface in the presence and absence of simulated solar light and a photosensitizer. *Chemical Science*, 9(26), 5716–5723. <https://doi.org/10.1039/c8sc01957f>

Slade, J. H., Shiraiwa, M., Arangio, A., Su, H., Poschl, U., Wang, J., & Knopf, D. A. (2017). Cloud droplet activation through oxidation of organic aerosol influenced by temperature and particle phase state. *Geophysical Research Letters*, 44(3), 1583–1591. <https://doi.org/10.1002/2016GL072424>

Stemmler, K., Ndour, M., Elshorbany, Y., Kleffmann, J., D'Anna, B., George, C., et al. (2007). Light induced conversion of nitrogen dioxide into nitrous acid on submicron humic acid aerosol. *Atmospheric Chemistry and Physics*, 7(16), 4237–4248. <https://doi.org/10.5194/acp-7-4237-2007>

Stokes, M. D., Deane, G. B., Prather, K., Bertram, T. H., Ruppel, M. J., Ryder, O. S., et al. (2013). A marine aerosol reference tank system as a breaking wave analogue for the production of foam and sea-spray aerosols. *Atmospheric Measurement Techniques*, 6(4), 1085–1094. <https://doi.org/10.5194/amt-6-1085-2013>

Trueblood, J. V., Wang, X., Or, V. W., Alves, M. R., Santander, M. V., Prather, K. A., & Grassian, V. H. (2019). The old and the new: Aging of sea spray aerosol and formation of secondary marine aerosols through OH oxidation reactions. *ACS Earth and Space Chemistry*, 3(10), 2307–2314. <https://doi.org/10.1021/acsearthspacechem.9b00087>

Wang, X. F., Sultana, C. M., Trueblood, J., Hill, T. C. J., Malfatti, F., Lee, C., et al. (2015). Microbial control of sea spray aerosol composition: A tale of two blooms. *ACS Central Science*, 1(3), 124–131. <https://doi.org/10.1021/acscentsci.5b00148>

Yang, Y., & Nagata, T. (2021). Viral production in seawater filtered through 0.2-μm pore-size filters: A hidden biogeochemical cycle in a neglected realm. *Frontiers in Microbiology*, 12, 774849. <https://doi.org/10.3389/fmicb.2021.774849>

Zimmermann, R. (1977). Estimation of bacterial number and biomass by epifluorescence microscopy and scanning electron microscopy. In G. Rheinheimer (Ed.), *Microbial ecology of a brackish water environment* (pp. 103–120). Springer Berlin Heidelberg.

Zsolnay, A., Baigar, E., Jimenez, M., Steinweg, B., & Saccamandi, F. (1999). Differentiating with fluorescence spectroscopy the sources of dissolved organic matter in soils subjected to drying. *Chemosphere*, 38(1), 45–50. [https://doi.org/10.1016/S0045-6535\(98\)00166-0](https://doi.org/10.1016/S0045-6535(98)00166-0)